3 Comparative Ratings and Properties

3.1 SYSTEM RATINGS

In order to design an appropriate storage device and to choose the right solution in relation to a given application, it is important to have a comparative evaluation of its possible capacity and performance. First, the power range must be defined. Then, with respect to the necessary autonomy, the energy capacity can be defined. Figure 3.1 is a representation of a high number of possible solutions over a large power range of six decades, starting from the 1 kW level up to the GW level. Different storage technologies are presented, from electrochemical batteries to large-scale pumped hydro storage. Compressed air energy storage (CAES), superconductive magnet energy storage (SMES), and flywheels are compared. The vertical axis of the figure illustrates the system autonomy, in powers of 10 h. The product of the power multiplied by the time gives the energy capacity. This parameter corresponds to the surface delimited by the horizontal and vertical lines of the represented values in the diagram. A conventional approach considers real systems related to a possible autonomy of up to tens of hours. These technologies are represented in the lower half of Figure 3.1. For longer storage times, the so-called seasonal storage, several possibilities exist that are based on complex transformations. In Figure 3.1, the long-term storage is represented up to 10^3 h. This indicative value could correspond to a transformation from solar power to hydrogen, defined over 3 months (100 days), and with a collection rate of up to 10 h/day.

3.2 ENERGY DENSITY

One important parameter related to a given technology is energy density. In Figure 3.2, the energy densities of several techniques are indicated [1]. On the vertical axis, the *weight energy density* is indicated.

The symbol used for the weight energy density is e_m [Wh/kg]

This parameter is generally indicated in Wh/kg, or in kWh/ton.

Another parameter for the energy density is the *volume energy density*.

The symbol used for the volume energy density is e_v [Wh/dm^3]

This parameter is indicated in kWh/m^3, or in Wh/dm^3.

These symbols are chosen according to recommendations of the International Electrotechnical Commission (IEC) [2].

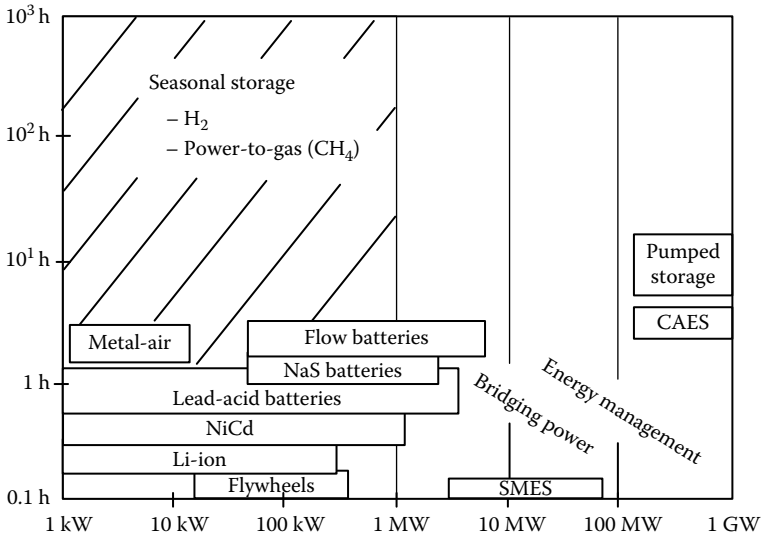

FIGURE 3.1 Overview on storage systems.

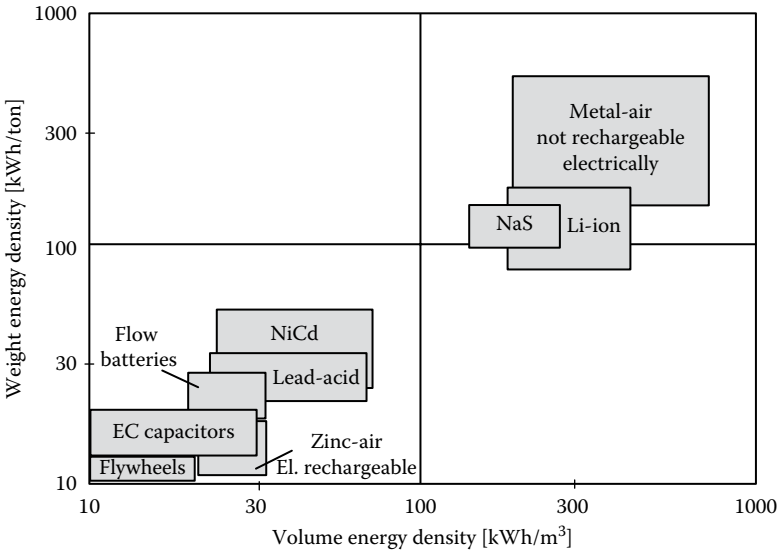

FIGURE 3.2 Weight and volume energy density.

The parameters on energy density are important with regard to the choice of technology for a given application.

Mobile applications are the most concerned by the weight energy density. In this context, an extreme case of application is the "Solarimpulse" project, which uses modern high-performance batteries in order to be able to fly overnight with energy accumulated during the day by photovoltaic (PV) cells placed on the airplane wings [3].

As will be shown in Section 3.5, the values of the energy density indicated by manufacturers are generally not considering any energy efficiency or losses during charging, discharging nor self-discharging losses. In reality, the stored energy corresponds to a given value that is not equal to what can be extracted. This last value depends on the power level of the energy exchange.

3.3 POWER DENSITY AND SPECIFIC POWER

A second method of comparing storage devices is to quantify their power capability. This is often given by the power density or by the specific power. The power density is the amount of power (time rate of energy transfer) per unit volume. It is also called the *volume power density*.

The symbol used for the power density is p_v [W/dm^3]

It is expressed in W/dm^3 or in kW/m^3. It is also possible to give the value of the volume power density in W/m^3, as can be found in some scientific tables [4].

The *power-to-weight ratio* or *specific power* is the power generated by a source divided by the mass.

The symbol used for the *power-to-weight ratio* is p_m [W/kg]

This parameter is given in W/kg or in kW/ton. For powerful devices such as supercapacitors or thermal generators, the specific power is often given in kW/kg.

As already mentioned in the previous section for the energy density, these parameters are only an indication given by the manufacturer to define what is possible or admissible for their use. The indicated values cannot be interpreted in the sense of energy efficiency.

3.4 RAGONE CHART

The Ragone chart is used for performance comparison of various energy storage devices (ESDs). The represented values on a Ragone chart are

- Specific energy or weight energy density (in Wh/kg) e_m

versus

- Specific power or power-to-weight ratio (in W/kg) p_m

The axes of a Ragone chart are logarithmic, which allow comparing the performance of very different devices (e.g., extremely high and extremely low power).

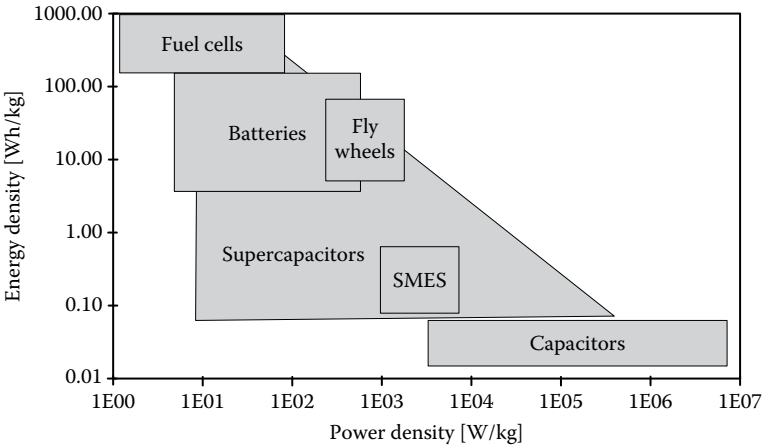

FIGURE 3.3 The Ragone chart.

Figure 3.3 gives an example of a Ragone chart used by one manufacturer for the positioning of a given technology in a general context of ESDs.

In this diagram, one can see that the vertical axis is labeled as energy density, more precisely the weight energy density (or specific energy) in Wh/kg [5].

3.5 THEORY OF RAGONE PLOTS

As described in Chapter 1, the energy efficiency of a storage device is related to the different losses. Charging and discharging losses as well as the self-discharge losses influence directly the round-trip efficiency. As a consequence, the amount of energy that can really be recovered from a fully charged storage device has to be defined depending on the instantaneous power of the energy transfer.

This principle of interdependency between the energy density and the power density is described by "the theory of Ragone plots" [6].

In this regard, a general circuit is associated with Ragone plots (Figure 3.4). The ESD feeds a load with constant power P. The ESD contains elements for energy storage. Due to constant power, energy supply occurs only for a finite time $t_{\text{inf}}(P)$. The energy available for the load E, depending on the power P, defines a Ragone plot.

Consider the general circuit of Figure 3.4. For example, the ESD may consist of a voltage source, $V(Q)$, depending on the stored charge Q, an internal resistor R, and an internal inductance L. Note that this ESD can describe many kinds of electric power sources. The ESD is connected to a load that draws a constant power $P \geq 0$. Such a load can be realized with an electronically controlled power converter feeding an external user. The current I and voltage U at the load are then related nonlinearly by $U = P/I$. Provided reasonable initial conditions

$$Q(0) = Q_0 \quad \text{and} \quad \dot{Q}(0) = \dot{Q}_0$$

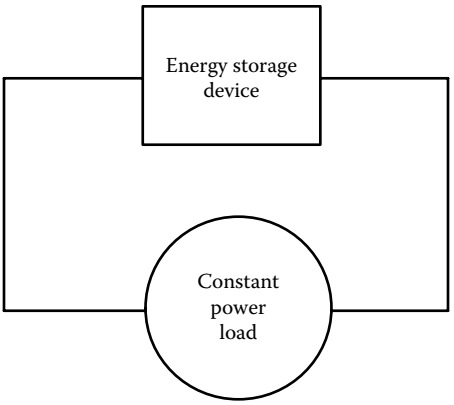

FIGURE 3.4 General circuit associated with Ragone plots. (Adapted from Christen, T. and Carlen, M.W., *J. Power Sources*, 91, 210, 2000.)

are given, the electrical dynamics is governed by the following ordinary differential equation:

$$L\ddot{Q} + R\dot{Q} + V(Q) = -\frac{P}{\dot{Q}} \tag{3.1}$$

where the dot indicates differentiation with respect to time.

This equation applies not only to electrical ESD but covers many kinds of physical systems (mechanical, hydraulic, etc.). Without making reference to a specific physical interpretation of Relation 3.1, the Ragone curve can be defined as follows: At time $t = 0$, the device contains the stored energy

$$E_0 = \frac{L\dot{Q}_0^2}{2} + W(Q_0) \tag{3.2}$$

For $t > 0$, the load draws a constant power P, such that $Q(t)$ satisfies Relation 3.1. It is clear that for finite E_0 and P, the ESD is able to supply this power only for a finite time, say $t_{\text{inf}}(P)$. A criterion is given either by when the storage device is cleared or when the ESD is no longer able to deliver the required amount of power. Since the power is time independent, the available energy is

$$E(P) = P \cdot t_{\text{inf}}(P) \tag{3.3}$$

The curve $E(P)$ versus P corresponds to the Ragone plot.

3.5.1 Ragone Plot of a Battery

In this section, the particular case of an ideal battery is studied. First, and regarding the model leading to the Relation 3.1, we assume the condition $L = 0$. Then, the ideal

battery with a capacity of Q_0 is characterized by a constant cell voltage $V = U_0$, if $Q_0 \geq Q > 0$ and $V = 0$, if $Q = 0$. In a first step, the leakage resistor R_L is neglected.

Relation 3.1 reads

$$P = U \cdot I = \left(U_0 - RI\right) I$$

where

U is the terminal voltage

$I = \dot{Q}$ is the current

The solutions of the quadratic equation are as follows:

$$I_{\pm} = \frac{U_0}{2R} \pm \sqrt{\frac{U_0^2}{4R^2} - \frac{P}{R}} \tag{3.4}$$

At the limit $P \to 0$, the two branches correspond to a discharge current:

$$I_+ \to \frac{U_0}{R} \quad \text{and} \quad I_- \to 0.$$

For the ideal battery, the constant power sink can also be parametrized by a constant load resistance R_{load}.

The two limits belong then to $R_{load} \to 0$ (short circuit) and $R_{load} \to \infty$ (open circuit), respectively.

Clearly, in the context of the Ragone plot, we are interested in the latter limit, such that we have to take the branch with the minus sign, $I \equiv I_-$ in Equation 3.2.

Now the battery is empty at time $t_{inf} = Q_0/I$, where the initial charge Q_0 is related to the initial energy $E_0 = Q_0 U_0$. It is now easy to include the presence of an ohmic leakage current into the discussion. The leakage resistance R_L increases the discharge current I by U_0/R_L.

The energy being available for the load becomes

$$E_b\left(P\right) = P \cdot t_\infty = \frac{2RQ_0P}{U_0 - \sqrt{U_0^2 - 4RP} + 2U_0R/R_L} \tag{3.5}$$

Equation 3.5 corresponds to the Ragone curve of the ideal battery. In the presence of leakage, $E_b(0) = 0$. For the extracted energy, there exists a maximum at

$$P = \frac{U_0^2}{\sqrt{2RR_L}}$$

Without leakage $R/R_L \to 0$, the maximum energy is available for vanishing low power $E_b(P \to 0) = E_0$. From Equation 3.5, one concludes that there is a maximum power, $P_{max} = \frac{U_0^2}{4R}$, associated with an energy $E_0/2$ (a small correction due to leakage is neglected).

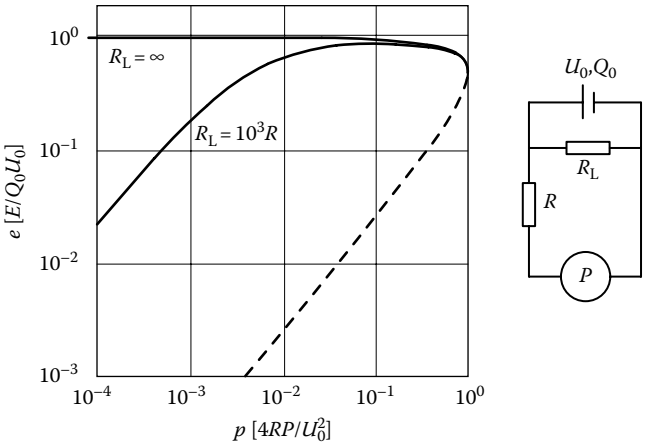

FIGURE 3.5 Ragone curve of the ideal battery. (Adapted from Christen, T. and Carlen, M.W., *J. Power Sources*, 91, 210, 2000.)

This point is the endpoint of the Ragone curve of the ideal battery, where only half of the energy is available, while the other half is lost at the internal resistance.

Finally, the expression of the Ragone plot is given in the dimensionless units using

$$e_b = \frac{E_b}{Q_0 U_0} \quad \text{and} \quad p = \frac{4RP}{U_0^2}$$

$$e_b(p) = \frac{1}{2}\frac{p}{\left(1 - \sqrt{1-p} + 2R/R_L\right)} \tag{3.6}$$

Ragone curves according to Equation 3.5, with and without leakage, are shown in Figure 3.5 for the ideal battery. The branch belonging to I_+ is plotted by the dashed curve.

3.5.2 Case of the Capacitor

In the case of an ideal electric capacitor (see Figure 3.6), an ordinary differential equation (ODE) rather than an algebraic equation has to be solved. The electric potential depends linearly on the charge via a capacitance C:

$$V(Q) = \frac{Q}{C}$$

According to the relative complex calculations given in Reference 6, the Ragone curve of a capacitor can be expressed by

$$E_c(P) = \frac{C}{2}\left(RP \ln\left(\frac{RP}{U_0^2}\right) + U_0^2 - RP\right) \tag{3.7}$$

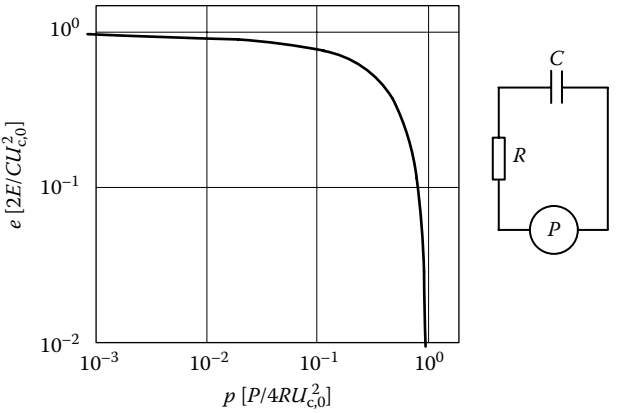

FIGURE 3.6 Normalized Ragone curve for the capacitor. (Adapted from Christen, T. and Carlen, M.W., *J. Power Sources*, 91, 210, 2000.)

$$U_0 = \frac{U_{C,0}}{2} + \sqrt{\frac{U_{C,0}^2}{4} - RP} \tag{3.8}$$

where the initial capacitor voltage $U_{C,0}$ is related to the total energy by E_0:

$$E_0 = \frac{CU_{C,0}^2}{2}$$

In the dimensionless units

$$e_c = \frac{2E_c}{CU_{C,0}^2} \tag{3.9}$$

and

$$p = \frac{2RCP}{E_0}$$

the Ragone curve reads

$$e_c(p) = \frac{1}{4}\left(\left(1+\sqrt{1-p}\right)^2 - p - p\ln\left(\frac{\left(1+\sqrt{1-p}\right)^2}{p}\right)\right) \tag{3.10}$$

and is represented in Figure 3.6.

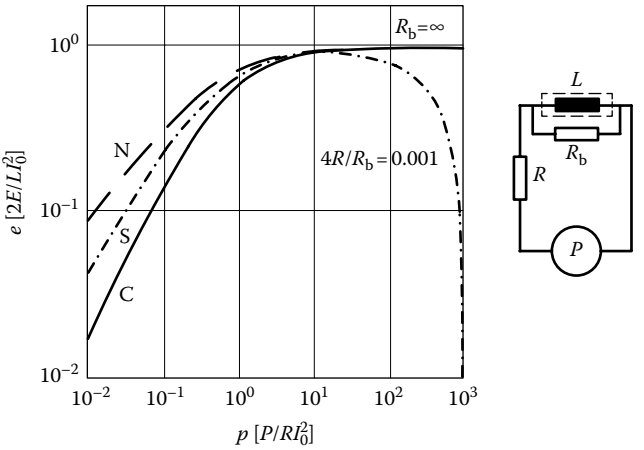

FIGURE 3.7 Normalized Ragone curves for the inductive ESD. (Adapted from Christen, T. and Carlen, M.W., *J. Power Sources*, 91, 210, 2000.)

3.5.3 Case of Superconductive Magnetic Energy Storage

The Ragone curves of SMES systems are also described in detail in Reference 6. Figure 3.7 gives the normalized curves for inductive ESDs with Coulomb (C), Stokes (S), and Newton (N) friction. The dashed double-dotted curve corresponds to an SMES with an ohmic bypass ($4R/R_b$ = 0.001). This resistance R_b is used for the modeling of the losses of all freewheeling paths, with a dominant contribution of the freewheeling elements of the power electronic converter (see Figure 2.4).

3.6 MODIFIED RAGONE REPRESENTATION

A similar method for representing the relation between the real energy capacity of a storage device and the charging/discharging power can be found in Reference 7. In this contribution, the question of the "amplification of power" is addressed.

Power amplification can be illustrated with the example of "waste compactors," known as the "Big Belly" [8] and represented in Figure 3.8b. In such special applications, a storage device is used to harvest energy at a low power level (e.g., P_1 = 10 W) and to feed an application with a much higher power (e.g., P_2 = 125 W, Figure 3.8a). Another example of power amplification through storage is described in Reference 9, where a direct connected supercapacitor is used as an energy buffer for a small PV generator.

In Reference 7, the model of the modified Ragone representation (MRR) is used. The ESD is represented as an ideal battery with series resistor R_s and a parallel connected leakage element R_p (Figure 3.9). The energy that can be recovered from the storage device is represented in the function of the transfer power P (logarithmic scale, Figure 3.10). Too less a power in the range of the self-discharge losses results in nearly zero energy recovered (left ends of the curves in Figure 3.10).

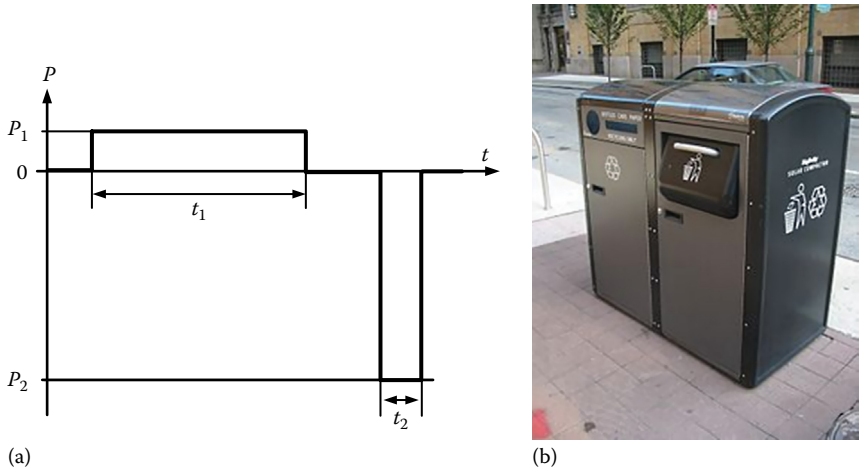

FIGURE 3.8 (a) Principle of charge and discharge (power amplification) and (b) example of a waste-compactor.

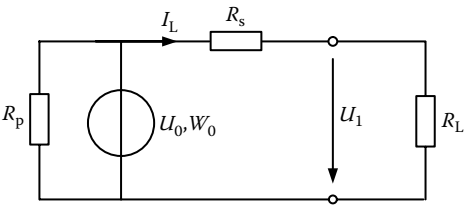

FIGURE 3.9 Equivalent scheme used for the modified Ragone representation (MRR).

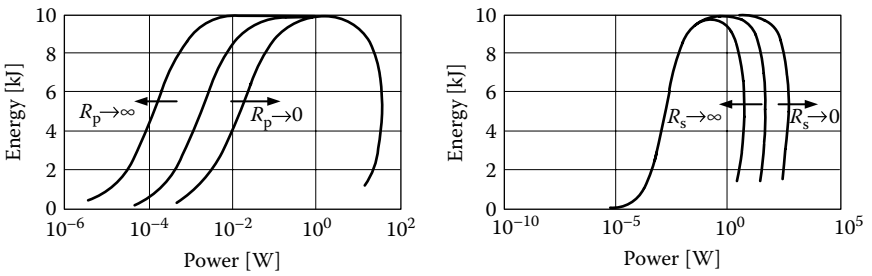

FIGURE 3.10 The modified Ragone representation (MRR). (Adapted from Delalay, S., Etude systémique pour l'alimentation hybride—Application aux systèmes intermittents, PhD thesis no. 5768, EPFL, Lausanne, Switzerland, 2013, https://infoscience.epfl.ch/record/187365/files/EPFL_TH5768.pdf, accessed on September 22, 2017.)

At the right end of the MRR curve, the effect of a too-high transfer power results in a similar situation of zero recovery.

The MRR given in Figure 3.10 corresponds to the same analysis as already presented in Section 3.5.1 but with a different formulation of the different powers. The boundary between the extracted current and the power provided to the load is given for the specified variables in Figure 3.9:

$$P_{\mathrm{L}} - U_0 I_{\mathrm{L}} + R_{\mathrm{s}} I_{\mathrm{L}}^2 = 0 \tag{3.11}$$

with

$$P_{\mathrm{L}} = R_{\mathrm{L}} I_{\mathrm{L}}^2 \tag{3.12}$$

Additionally, the losses in the self-discharge path and the internal dissipation are considered:

$$P_{\mathrm{p}} = \frac{U_0^{2\,2}}{R_{\mathrm{p\,L}}} \tag{3.13}$$

$$P_{\mathrm{s}} = \frac{1}{2R_{\mathrm{s}}} U_0 \left(U_0 - \sqrt{U_0^2 - 4P_{\mathrm{L}} R_{\mathrm{s}}} \right) - P_{\mathrm{L}} \tag{3.14}$$

Finally, for a constant power extracted from the storage device the really recovered amount of energy is given by

$$E_{\mathrm{recov}} = P_{\mathrm{L}} \frac{W_0}{P_{\mathrm{s}} + P_{\mathrm{L}} + P_{\mathrm{p}}} = \frac{P_{\mathrm{L}}}{U_0} \frac{2R_{\mathrm{s}} W_0}{U_0 \left(1 + \dfrac{2R_{\mathrm{s}}}{R_{\mathrm{p}}} \right) - \sqrt{U_0^2 - 4R_{\mathrm{s}} P_{\mathrm{L}}}\,)} \tag{3.15}$$

Further calculations for intermittent use of storage devices and also for different steps of the extracted power are given in Reference 7.

3.6.1 Power Amplification in Successive Stages

From Figure 3.8a, the power amplification factor (PAF) can be defined as the ratio of

$$\mathrm{PAF} = \frac{P_2}{P_1} \tag{3.16}$$

According to its MRR, the storage device used for achieving a given power amplification may be unsuitable in the sense of leading to an insufficient round-trip energy efficiency because of the too-narrow power zone of the MRR, or, in other words, where the zone of "good efficiency" is smaller than the desired PAF. In such a case,

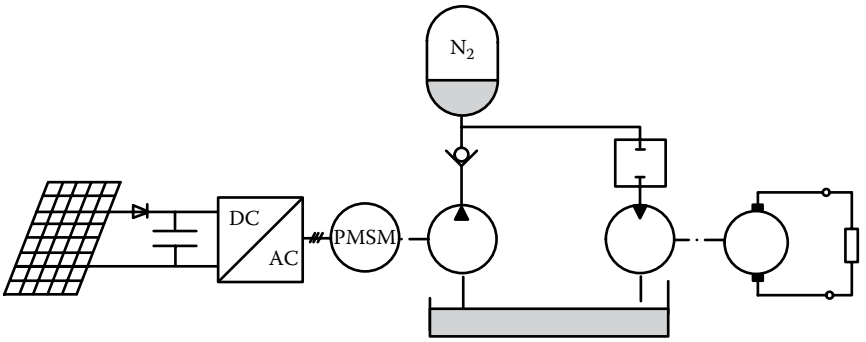

FIGURE 3.11 Energy harvesting system with two-stage accumulation.

the power amplification must be achieved in two successive steps. In Figure 3.11, a two-stage power amplification system is represented, where the input power is provided by a very small PV generator. The first stage of the power amplification system uses a supercapacitor directly connected to the PV generator. From this supercapacitor storage device, a higher power is used to periodically charge a second accumulation stage where a hydraulic bladder is fed with oil using a small motor and pump. Then, for the final application, the hydraulically stored energy can be used with a much higher power level.

In Figure 3.12, the MRR of the two stages are represented, namely, the supercapacitor (black traced line) and the hydraulic accumulator (full line). The dotted curves represent the properties of the PV panels, when the solar radiation varies and

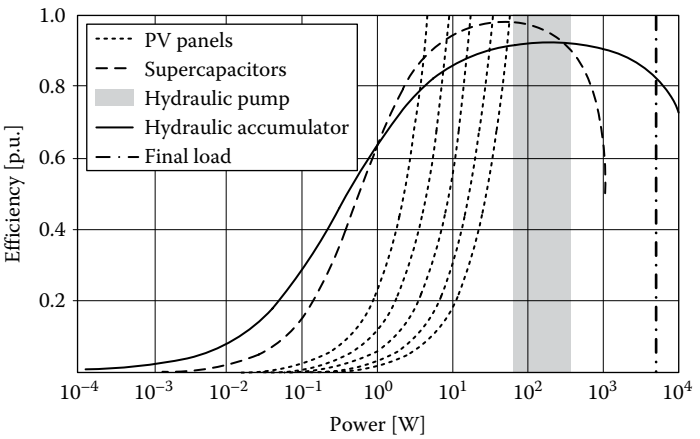

FIGURE 3.12 Modified Ragone representation (MRR) of a two-stage power amplification system. (Adapted from Delalay, S., Etude systémique pour l'alimentation hybride—Application aux systèmes intermittents, PhD thesis no. 5768, EPFL, Lausanne, Switzerland, 2013, https://infoscience.epfl.ch/record/187365/files/EPFL_TH5768.pdf, accessed on September 22, 2017.)

the maximum power point tracking (MPPT) control circuit sets the operating point (power between 2 and 50 W). The vertical mixed line represents the power required by the final application (5 kW). This power level can be supplied by the hydraulic accumulator, while the supercapacitor would show a nearly zero efficiency at that value of the power. The gray zone in Figure 3.12 illustrates the variable power required for the charging of the hydraulic accumulator due to the variation of its internal gas pressure. The intersections between this gray zone and the MRRs of both the supercapacitor and the hydraulic accumulator define energy transfers between the stages with an acceptable efficiency above 80%. This value comprises the losses of the discharge of the first stage, together with the losses of charging of the second stage.

It appears in Figure 3.12 that from the point of view of the MMRs of the storage devices only, an acceptable intersection domain between the PV panels and the hydraulic accumulator would be possible (intersection of the PV curves and the hydraulic accumulator's MRR, left from the green zone). However, the energy efficiency of the needed hydraulic pump intervenes also in the global account. Here, the operating power of this pump must be kept over a minimum value in order to get an acceptable efficiency of that additional intermediary conversion stage.

3.7 TYPICAL EFFICIENCIES, LIFETIME, AND COSTS

Figure 3.13 illustrates the efficiencies and lifetimes of different storage technologies. These parameters are of high importance, especially in a context where the "energy economy" factors intervene. Classical as well as modern batteries show very good energy efficiencies, but they suffer from limited life cycles or lifetimes in the range of only several hundreds to several thousands of cycles, which is a limiting factor in the

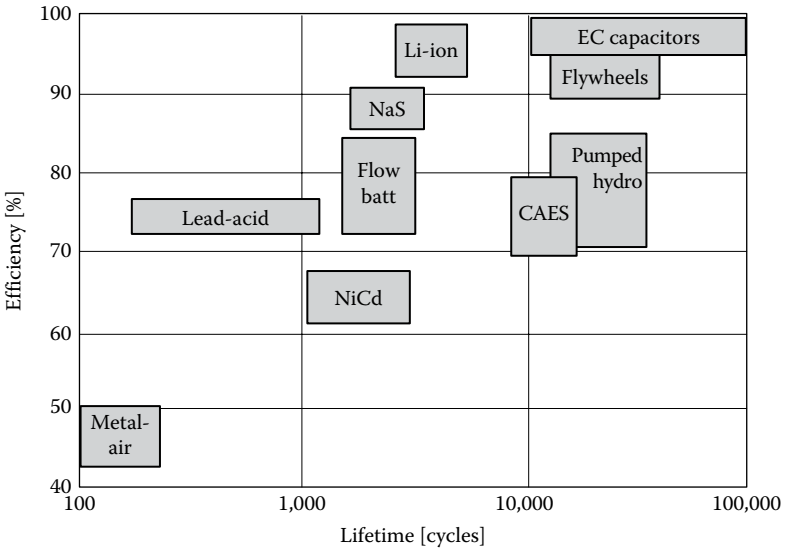

FIGURE 3.13 Efficiency and lifetime of different storage technologies.

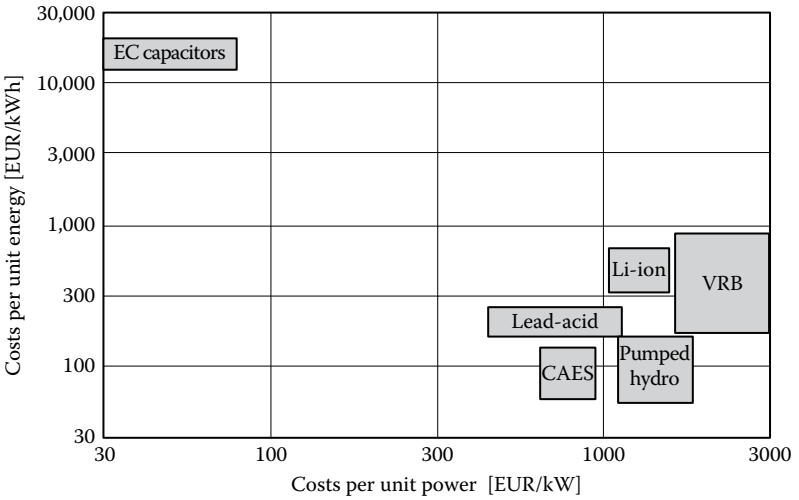

FIGURE 3.14 Capital costs of storage solutions.

domain of renewable energy sources. On the right side of Figure 3.13, technologies with higher numbers of possible cycles are represented. They generally belong to the category of solutions based on reversible physics.

Figure 3.14 indicates the capital costs related to different storage solutions. This representation is related to the time and evolution of the costs of the technologies. Especially the costs of new techniques must be periodically reevaluated. The criteria for selection of a given technology must be evaluated together with the technical performance criteria like the lifetime and efficiency, as well as the context of utilization [10–12].

A more realistic economic model for evaluation or comparison of a storage solution should take into account the costs of the storage infrastructure, the lifetime of the system, as well as its efficiency (Relation 3.17).

$$\text{Real\_costs} = \frac{\text{Capital/Energy}}{\text{Lifetime} \cdot \text{Efficiency}} \tag{3.17}$$

EXERCISE 1: NORMAL AND FAST CHARGE OF BATTERIES IN EVS—THE QUESTION OF ENERGY EFFICIENCY

Modern batteries claim high C-rates up to factors 8 (short-term 15), which could make possible fast charge in the electric vehicle (EV) applications. A system is studied where the energy can be collected from PV panels and prestored during the day. The energy transfer from the local battery to the vehicle battery at the end of the day can then be realized in a longer or shorter time (Figure 3.15). Even if no PV panels are used, the precharge of the local battery is done from grid electricity, and the role

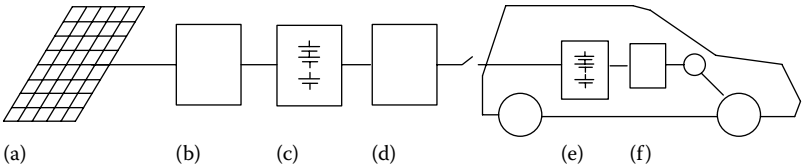

FIGURE 3.15 EV charging from RES (PV). (a) PV panels, (b) MPPT converter, (c) local battery, (d) DC–DC converter, (e) car battery, and (f) propulsion system.

of that local battery will be to serve as a buffer, avoiding the high power solicitation from the grid during the fast charge (high power) of the EV battery.

The batteries present, however, not negligible internal resistance, and the energy transfer is affected by losses. The student must investigate the PV collection system and panels, the precharge and fast transfer mechanism, and design suited accumulators. Especially the energetic properties must be illustrated (e.g., the efficiency as a function of the transfer time).

Technical Parameters

Local Battery

The local battery is realized with 135 elements of 3.7 V and 0.7 mΩ internal resistance.

No-load voltage of the local battery: 500 V.

The local battery energy capacity is equal to 25 kWh.

From the nominal capacity of the elements (50 Ah) the rated current is defined as 50 A, corresponding to a *C*-factor equal to 1 (under $C = 1$ conditions, the charging time is equal to 1 h).

Car Battery

The car battery is realized with 108 elements of 3.7 V and 0.7 mΩ internal resistance (identical elements as for the local battery).

No-load voltage of the car battery: 400 V.

Converter Losses

The converter losses are calculated through the conduction loss of the silicon devices with a forward voltage of the devices (transistors and diodes) equal to 1.5 V. More details are to be found in Section A.3.1.1.

PV Panels

The PV panel surface is designed according a charging time of the local battery within 7 h, from SOC 20% to full charge (SOC = 100%).

The required panel surface must be calculated for the following conditions:

$\varepsilon = 800\ \text{W/m}^2$ (mean value)

$\eta_{\text{cells}} = 10\%$

Structure of the System, Converters, and Cascaded Conversions

The electric scheme of the system with the different converters should be drawn.

a. Slow charge (7 h)
   The current in both the PV panels and the local battery should be "nondiscontinuous." It is smoothed with inductors:
   $L = 9.15$ mH, $R_L = 0.2\ \Omega$
b. Fast energy transfer from the local battery to the car battery (C-rate = 8).
   In order to reduce costs, there is only one converter for both batteries (step-down converter). The current in the car battery is smoothed with an inductor:
   $L = 9.15$ mH, $R_L = 0.32$ mΩ

Energy Efficiency

a. Calculate the energy efficiency of a charge from the PV panels (slow charge, 7 h). For this case (a), there is a step-up converter cascaded with a step-down converter. Between the two converters, there is a constant DC voltage link based on a buffer capacitor.
   The energy efficiency is calculated on the base of the different power losses (converters, smoothing inductors, internal losses of the battery).
b. Calculate the energy efficiency of a charge of the car battery (from the local battery, case b), for different charging times (using the C-rates of 2, 4, 6, 8, 10, 12).
   The goal of this exercise is to set in evidence the importance of the different losses, to show what components have the most influence on the efficiency, and to show how the losses are depending on the charging speed.

SOLUTION TO EXERCISE 1

Model of the Local Battery

The local battery can be modeled through the equivalent scheme of Figure 3.16.
The battery no-load voltage is

$$U_{b\_loc} = 135 \cdot 3.7\ \text{V} = 499.5\ \text{V} \tag{3.18}$$

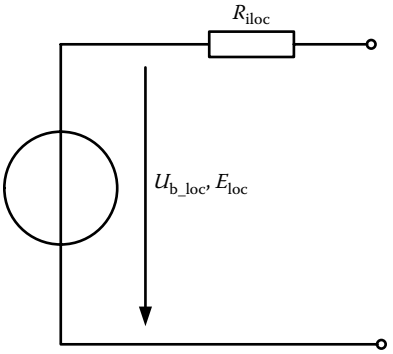

FIGURE 3.16 Simplified model of the local battery.

The internal resistance is

$$R_{\mathrm{i\_loc}} = 135 \cdot 0.7 \ \mathrm{m\Omega} = 0.095 \ \Omega \tag{3.19}$$

The battery energy capacity is

$$E_{\mathrm{loc}} = 50 \ \mathrm{Ah} \cdot 499.5 \ \mathrm{V} = 24.975 \ \mathrm{kWh} \tag{3.20}$$

Model of the Car Battery

The car battery can be modeled through the equivalent scheme of Figure 3.17.

The battery no-load voltage is

$$U_{\mathrm{b\_car}} = 108 \cdot 3.7 \ \mathrm{V} = 399.6 \ \mathrm{V} \tag{3.21}$$

The internal resistance is

$$R_{\mathrm{i\_car}} = 108 \cdot 0.7 \ \mathrm{m\Omega} = 0.076 \ \Omega \tag{3.22}$$

The battery energy capacity is

$$E_{\mathrm{car}} = 50 \ \mathrm{Ah} \cdot 399.6 \ \mathrm{V} = 19.980 \ \mathrm{kWh} \tag{3.23}$$

PV Panels

The slow charge (7 h) of 80% of the (local) battery capacity defines the charging power:

$$P_{80\%} = \frac{0.8 \cdot 24.975 \ \mathrm{kWh}}{7 \ \mathrm{h}} = 2.85 \ \mathrm{kW} \tag{3.24}$$

The solar (irradiance) power is consequently

$$P_{\mathrm{sol}} = \frac{P_{80\%}}{\eta} = \frac{2.85 \ \mathrm{kW}}{0.1} = 28.5 \ \mathrm{kW} \tag{3.25}$$

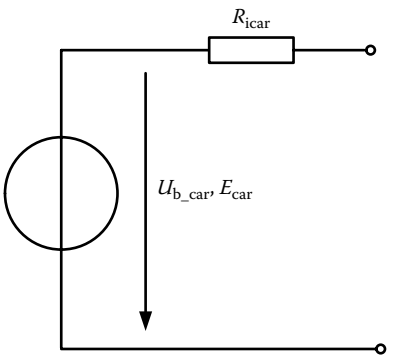

FIGURE 3.17 Simplified model of the car battery.

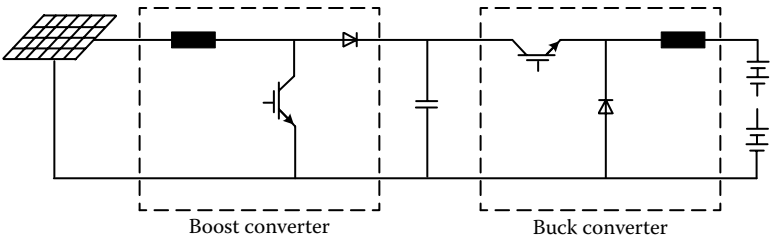

FIGURE 3.18 Charging system of the local battery from PV panels.

For a simplified design of the PV generator, the supposition is made that the solar irradiance is of a constant average value of 800 W/m^2 during 7 h. The PV panel surface becomes

$$S_{PV} = \frac{28.5\ \text{kW}}{800\ \text{W/m}^2} = 35.7\ \text{m}^2 \tag{3.26}$$

Charging in 7 h

The scheme of the charging system (slow charge) is given in Figure 3.18.

The charging current is calculated as (80% of battery capacity in 7 h):

$$I_{ch} = \frac{0.8 \cdot 50\ \text{Ah}}{7\ \text{h}} = 5.71\ \text{A} \tag{3.27}$$

In the system represented in Figure 3.18, the power produced by the PV panels is transferred to the intermediate DC circuit with the help of the boost converter. This converter assumes the function of the adaptation of the voltage of the panels to a constant DC voltage. In addition, this converter allows the optimal operation of the PV panels at their point of maximum power (MPPT).

The characteristic curves of the PV panels are represented in Figure 3.19. The voltage of the intermediate DC circuit is also represented (U_{DC} = 550 V). This value allows the boost converter to be operated with any value of the voltage of the PV panels. The represented MPP point corresponds to maximum of power under a solar irradiance of $\varepsilon = 1$ and a temperature $\theta = 0°$.

From the intermediate circuit, the power is transferred to the local battery using the buck converter. This converter assumes the transfer of power under constant current control.

The typical waveforms of the boost and buck converters can be found in Sections A.3.1 and A.3.2.

The use of the cascade of a boost and of a buck converter implies a slightly reduced energy efficiency due to the double conversion. But the main advantage is that the current at both the input and the output sides is nondiscontinuous.

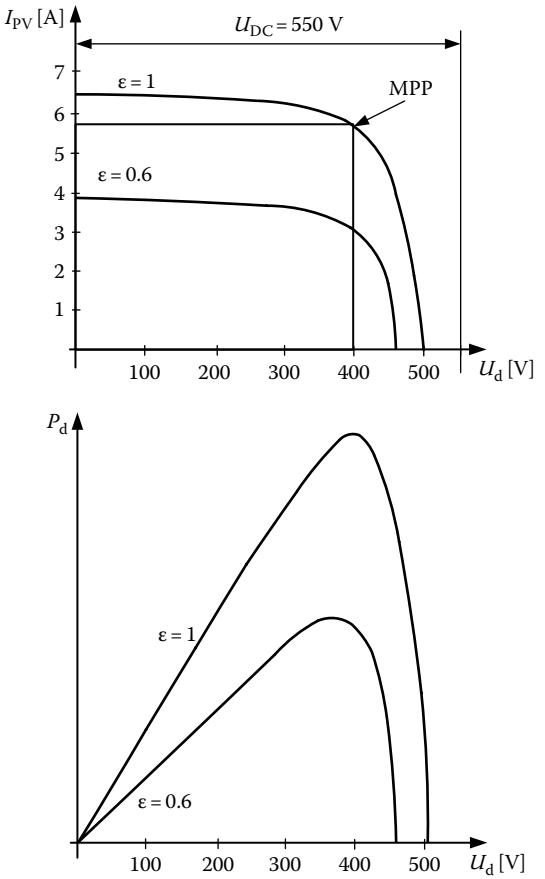

FIGURE 3.19 Characteristics of the PV panels.

The charging system with buck and boost converters is affected by power losses in the following elements (simplified estimation):

- Ohmic losses in the inductors
- Conduction losses in the power semiconductors of the boost and buck converters
- Ohmic losses in the battery

For the estimation of the losses, it is considered that the PV panels are operated at a voltage level corresponding approximately to the voltage level of the local battery. As a consequence, one can suppose the input current of the boost converter being identical to the output current of the buck converter.

The losses in the inductor of the boost converter are calculated as follows:

$$\text{Loss}_{\text{Lboost}} = R_{\text{L}} \cdot I^2 = 0.2\ \Omega \cdot \left(5.71\ \text{A}\right)^2 = 6.5\ \text{W} \tag{3.28}$$

The losses in the buck inductor are calculated as follows:

$$\text{Loss}_{\text{Lbuck}} = R_{\text{L}} \cdot I^2 = 0.2\ \Omega \cdot \left(5.71\ \text{A}\right)^2 = 6.5\ \text{W} \tag{3.29}$$

For the conduction losses in the converters, Relations A.6 and A.7 are used:

$$P_{\text{cond}} = P_{\text{onT}} + P_{\text{onD}} = U_{\text{CEon}} I_{\text{T}} + U_{\text{Don}} \cdot I_{\text{D}} = 1.5\ \text{V} \cdot 5.71\ \text{A} = 8.5\ \text{W} \tag{3.30}$$

(The on-state voltages of the diode and of the transistor are identical, and the on-state durations of these elements are complementary. Their sum is equal to 1; see (A.8))

The ohmic losses in the battery are given by

$$\text{Loss}_{\text{battery}} = R_{\text{iloc}} \cdot I^2 = 0.095\ \Omega \cdot \left(5.71\ \text{A}\right)^2 = 3.1\ \text{W} \tag{3.31}$$

The total transfer losses are then

$$\begin{aligned} \text{Loss}_{\text{transf}} &= \text{Loss}_{\text{Lboost}} + \text{Loss}_{\text{Lbuck}} + P_{\text{cond\_boost}} + P_{\text{cond\_bucl}} + \text{Loss}_{\text{batt}} \\ &= 6.5\ \text{W} + 6.5\ \text{W} + 8.5\ \text{W} + 8.5\ \text{W} + 3.1\ \text{W} = 33.1\ \text{W} \end{aligned} \tag{3.32}$$

The efficiency of the charging process is further

$$\eta = \frac{P_{\text{ch}}}{P_{\text{ch}} + \text{Loss}_{\text{transf}}} = \frac{2850\ \text{W}}{2850\ \text{W} + 33.1\ \text{W}} = 0.989 \tag{3.33}$$

Fast Charge from the Buffer

It is assumed that the car battery as well as the buffer (local) battery can be overloaded with a factor of 8C.

The car battery is then

$$I_{\text{car\_batt}} = 8 \cdot 50\ \text{A} = 400\ \text{A} \tag{3.34}$$

For the fast transfer from the local battery to the car battery, the scheme given in Figure 3.20 is chosen.

Figure 3.20 shows the use of a single buck converter. This choice is made on the basis of economic considerations.

To estimate the energy efficiency of the fast charge, the following elements are considered:

- Ohmic losses in the local battery
- Ohmic losses in the car battery
- Conduction losses in the power semiconductors

The ohmic losses in the inductor are neglected.

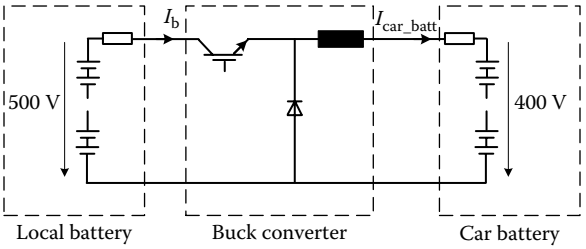

FIGURE 3.20 Scheme for the fast charge from the buffer battery.

For the calculation of the losses in the local battery, its current must be calculated. This current depends on the duty cycle of the buck converter corresponding to the ratio of the input to the output voltages:

$$I_e = \left(\frac{U_o}{U_e}\right) \cdot I_o = D \cdot I_o \quad \left(\text{see Relation A.5}\right) \tag{3.35}$$

The scheme of Figure 3.21 can be used as follows:

$$\left(U_{bloc} - R_{iloc} \cdot I_e\right) \cdot D = U_{bcar} + R_{icar} \cdot I_o \tag{3.36}$$

$$U_{bloc} \cdot D - D^2 R_{iloc} \cdot I_o = U_{bcar} + R_{icar} \cdot I_o$$

$$-D^2 R_{iloc} \cdot I_o + U_{bloc} \cdot D - \left(U_{bcar} + R_{icar} \cdot I_o\right) = 0 \tag{3.37}$$

$$D = \frac{-U_{bloc} \pm \sqrt{\left(U^2_{bloc} - 4R_{iloc} I_o \left(U_{bcar} + R_{icar} \cdot I_o\right)\right.}}{-2R_{iloc} I_o} \tag{3.38}$$

with the numerical values

$$D = \frac{-500\ \text{V} \pm \sqrt{\left(500\ \text{V}\right)^2 - 4 \cdot 0.095\ \Omega \cdot 400\ \text{A}\left(400\ \text{V} + 0.076\ \Omega \cdot 400\ \text{A}\right)}}{-2 \cdot 0.095\ \Omega \cdot 400\ \text{A}} = 0.926 \tag{3.39}$$

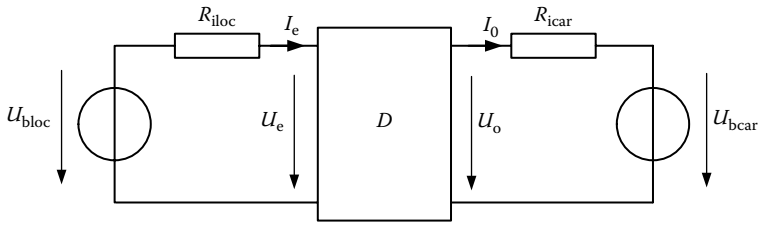

FIGURE 3.21 Equivalent scheme of the fast charge.

The second solution of the quadratic equation corresponds to a value of $D = 15$, which is incompatible with the normal operation of a buck converter. It must be ignored.

The current in the local battery is

$$I_e = D \cdot I_o = 0.926 \cdot 400 \text{ A} = 370 \text{ A} \tag{3.40}$$

And the losses in the local battery:

$$\text{Loss}_{l\_batt} = R_{iloc} \cdot I_e^2 = 0.095 \ \Omega \cdot (370 \text{ A})^2 = 13{,}032 \text{ W} \tag{3.41}$$

The losses in the car battery:

$$\text{Loss}_{car\_batt} = R_{icar} \cdot I_0^2 = 0.076 \ \Omega \cdot (400 \text{ A})^2 = 12{,}160 \text{ W} \tag{3.42}$$

The conduction losses in the semiconductors:

$$\text{Loss}_{converter} = U_{CEon} \cdot I_T + U_{Don} \cdot I_D = 1.5 \text{ V} \cdot 400 \text{ A} = 600 \text{ W} \tag{3.43}$$

The total losses related to the fast charge are consequently

$$\begin{aligned} \text{Loss}_{total} &= \text{Loss}_{lbatt} + \text{Loss}_{car\_batt} + \text{Loss}_{converter} \\ &= 13{,}032 \text{ W} + 12{,}160 \text{ W} + 600 \text{ W} = 25{,}792 \text{ W} \end{aligned} \tag{3.44}$$

Transferred Power

The power related to the fast charge is calculated. This value corresponds to the power that is really accumulated in the car battery:

$$P_{fast\_ch} = U_{bcar} \cdot I_o = 400 \text{ A} \cdot 400 \text{ V} = 160{,}000 \text{ W} = 160 \text{ kW} \tag{3.45}$$

Finally, the efficiency of the fast charge is given by

$$\eta_{fast\_ch} = \frac{P_{fast\_ch}}{P_{fast\_ch} + \text{Loss}_{total}} = \frac{160 \text{ kW}}{160 \text{ kW} + 25.8 \text{ kW}} = 0.86 \tag{3.46}$$

This value of efficiency corresponds to a charging current of 400 A. With this value of current, the car battery is charged within a time equal to

$$t_{charge} = \frac{\text{C\_capacity}}{I_{charge}} = \frac{50 \text{ Ah}}{400 \text{ A}} \cdot 60 \text{ min/h} = 7.5 \text{ min} \tag{3.47}$$

Figure 3.22 shows the value of the efficiency as a function of the battery charging time.

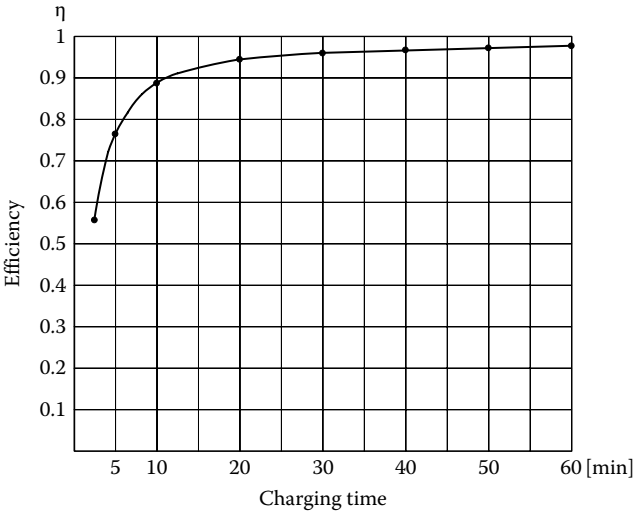

FIGURE 3.22 Efficiency as a function of the charging time.

EXERCISE 2: KINETIC ENERGY RECOVERY SYSTEM

The kinetic energy recovery system (KERS) is a power assistance system based on the recovery of a moving vehicle's kinetic energy under braking (Figure 3.23). The recovered energy is stored in a reservoir for later reuse under acceleration. Such systems have been developed for race cars based on different storage technologies. A first example using supercapacitors is described in Reference 13 and was developed under the label of "Formula S2000."

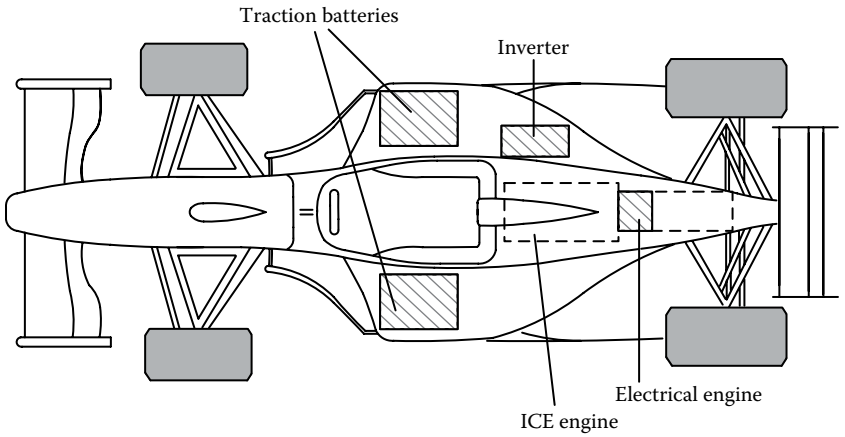

FIGURE 3.23 Power-assisted race car (Formula S2000).

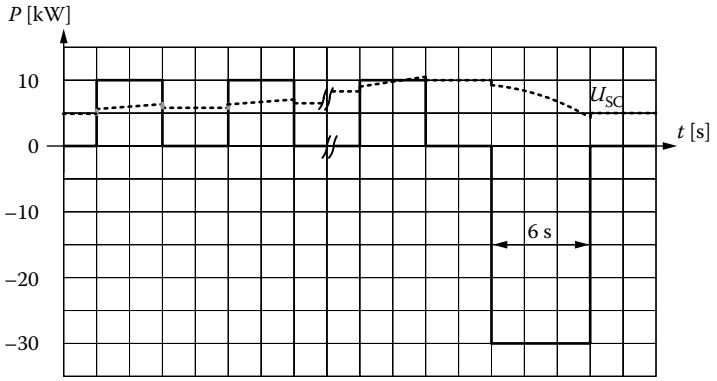

FIGURE 3.24 Power profile.

In this study, a supercapacitor-based storage system was chosen. It makes possible the recovery of successive small amounts of braking energy before allowing the driver to benefit from an additional acceleration power through a function called "push-to-pass."

The profile of the power recovered into the storage device is represented in Figure 3.24, together with the typical power impulse reused for acceleration. The voltage of the supercapacitors U_{SC} is also represented.

The power profile shows braking recovery impulses of 10 kW followed by an acceleration power of −30 kW. The duration of the additional acceleration is specified to 6 s.

The objective of the exercise is to evaluate the energy efficiency of the described design using supercapacitive storage for its discharge and to compare the result with another design using a Li-ion battery.

1. Calculate the maximum and minimum energy efficiency of the described solution using supercapacitors.
   The maximum efficiency corresponds to the case where the supercapacitors are fully charged, and the minimum to the case where the supercapacitor voltage is the lowest and where simultaneously the discharge current is the highest when the discharge occurs under constant power.
   Technical data:
   - Supercapacitors:
     Maxwell, $C = 310$ F, $R_i = 0.4$ mΩ, $U = 2.7$ V
   - Acceleration power (boost power): 30 kW
   - Energy capacity of the storage device: $E = 180{,}000$ J for a minimum voltage of 50% (selected for an additional power of 30 kW during 6 s).

   With the goal to illustrate the influence of the power level on the efficiency of the discharge, repeat the calculation of the minimum and maximum efficiency for discharge powers of 15, 6, and 3 kW.
   The values of the efficiency can now be represented graphically in an MRR (logarithmic scale for the power level). For the different power levels, the

TABLE 3.1
Parameters of the Li-Ion Battery

V	C	I_{dchmax}	R_i	m
3.3 V (2…3.6 V)	2.3 Ah	120 A (10 s)	10 mΩ	70 g

different values of the efficiency can be represented by vertical segments illustrating the domain between the minimum and maximum values.
For the logarithmic scale: log10 (2) ~ = 0.3, log10 (5) ~ = 0.7

2. Calculate the energy efficiency of a storage device realized with a Li-ion battery. The technical data of the Li-ion battery can be found in Table 3.1.
The design of the storage device must especially take into account that the Li-ion battery elements have a limited discharge current. This will lead to an oversize of the energy capacity.
Represent the properties of this storage device (Li-ion) in an MRR (P = 30, 15, 6, 3 kW).
Reference 10 indicates the difficulty to get real values on the internal resistance of commercial batteries and includes a method for evaluating this parameter.

SOLUTION TO EXERCISE 2

1. **Design with supercapacitors**
The energy stored in a supercapacitor charged at its maximum voltage is calculated as follows:

$$E = \frac{1}{2} C \cdot U_{\max}^2 = \frac{1}{2} \cdot 310 \text{ F} \cdot (2.7 \text{ V})^2 = 1129 \text{ J} \tag{3.48}$$

The remaining amount of energy after discharge down to 50% of the voltage is

$$E = \frac{1}{2} C \cdot U_{\min}^2 = \frac{1}{2} \cdot 310 \text{ F} \cdot (1.35 \text{ V})^2 = 882 \text{ J} \tag{3.49}$$

The extracted amount of energy becomes

$$E_{\text{disch}} = \frac{1}{2} C \cdot U_{\max}^2 - \frac{1}{2} C \cdot U_{\min}^2 = 1129 \text{ J} - 882 \text{ J} = 847 \text{ J} \tag{3.50}$$

The number of supercapacitors to be used for a total capacity of 180 kJ is then

$$N_{sc} = \frac{E_{\text{tot}}}{E_{\text{disch\_sc}}} = \frac{180{,}000 \text{ J}}{847 \text{ J}} = 212.5 \Rightarrow 213 \tag{3.51}$$

The maximum voltage of the storage device (all elements connected in series) becomes

$$U_{\max} = N_{\text{sc}} \cdot U_{\text{maxsc}} = 213 \cdot 2.7 \text{ V} = 575 \text{ V} \tag{3.52}$$

For a power delivery of 30 kW, the current in the supercapacitors is

$$I_{\min 30} = \frac{30 \text{ kW}}{575 \text{ V}} = 52.2 \text{ A} \tag{3.53}$$

At the end of the discharge with constant power, the current takes the value of

$$I_{\max 30} = \frac{30 \text{ kW}}{575 \text{ V} \cdot 0.5} = 104.4 \text{ A} \tag{3.54}$$

For the calculation of the efficiency, the following relation is used:

$$\eta = \frac{U_{\text{sc}} \cdot I_{\text{sc}} - R \cdot I_{\text{sc}}^2}{U_{\text{sc}} \cdot I_{\text{sc}}} = \frac{U_{\text{sc}} - R \cdot I_{\text{sc}}}{U_{\text{sc}}} \tag{3.55}$$

The voltage drop on the internal resistance of the supercapacitors must be calculated.
For the whole storage device (213 elements in series)

$$\begin{aligned} U_{\text{Rsc\_tot\_min}} &= R_{\text{sc}} \cdot I_{\text{sc}} \cdot N_{\text{sc}} = 0.4 \text{ m}\Omega \cdot 52.2 \text{ A} \cdot 213 \\ &= 4.45 \text{ V for the lowest current} \end{aligned} \tag{3.56}$$

and

$$\begin{aligned} U_{\text{Rsc\_tot\_max}} &= R_{\text{sc}} \cdot I_{\text{sc}} \cdot N_{\text{sc}} = 0.4 \text{ m}\Omega \cdot 104.4 \text{ A} \cdot 213 \\ &= 8.9 \text{ V for the highest one.} \end{aligned} \tag{3.57}$$

The corresponding efficiencies are then

$$\eta_{\text{max\_30}} = \frac{U_{\text{sc}} - R \cdot I_{\text{sc}}}{U_{\text{sc}}} = \frac{575 \text{ V} - 4.45 \text{ V}}{575 \text{ V}} = 0.992 \tag{3.58}$$

$$\eta_{\text{min\_30}} = \frac{U_{\text{sc}} - R \cdot I_{\text{sc}}}{U_{\text{sc}}} = \frac{575 \text{ V} \cdot 0.5 - 8.9 \text{ V}}{575 \text{ V} \cdot 0.5} = 0.969 \tag{3.59}$$

For a discharge at reduced power, only the minimal value of the efficiency is calculated. It has to be evaluated at the lower limit of the supercapacitor's voltage after discharge.
The extracted energy after a 15 kW impulse during 6 s is

$$E_{\text{extr\_15}} = 15{,}000 \text{ W} \cdot 6 \text{ s} = 90{,}000 \text{ J} \tag{3.60}$$

leading to the state of energy of one element of

$$E_{sc\_fin\_15} = 1129\ \text{J} - \frac{90{,}000\ \text{J}}{213} = 706\ \text{J} \tag{3.61}$$

the corresponding voltage of the elements being

$$U_{sc\_min\_15} = \sqrt{\frac{2E_{sc\_fin\_15}}{C}} = \sqrt{\frac{2 \cdot 706\ \text{J}}{310\ \text{F}}} = 2.13\ \text{V} \tag{3.62}$$

At this point, the discharge current is

$$I_{max\_15} = \frac{15{,}000\ \text{W}}{213 \cdot 2.13\ \text{V}} = 33\ \text{A} \tag{3.63}$$

leading to an efficiency of

$$\eta_{min\_15} = \frac{U_{sc} - R \cdot I_{sc}}{U_{sc}} = \frac{2.13\ \text{V} - 0.4 \cdot 10^{-3}\ \Omega \cdot 33\ \text{A}}{2.13V} = 0.993 \tag{3.64}$$

The efficiency is recalculated for the lowest values of the power (6 and 3 kW) and is represented in Figure 3.25.

Figure 3.25 shows that the design of the storage device on the base of supercapacitors presents an MRR where the efficiency is of high value (above 96%) within a full decade of the power level of the discharge, between 10% and 100% of the nominal power.

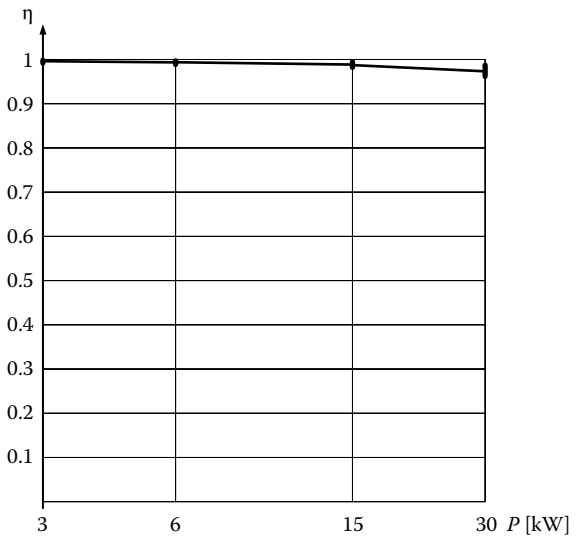

FIGURE 3.25 Efficiency (MRR) of the discharge of the supercapacitor-based storage device.

2. **Design with a Li-ion battery**
Parameters of the battery element:

$U = 3.3$ V
$C = 2.3$ Ah

The energy content of such an element is

$$E_{\text{batt}} = U \cdot C = 3.3\ \text{V} \cdot 2.3\ \text{Ah} = 3.3 \cdot 2.3 \cdot 3600\ \text{Ws} = 27{,}324\ \text{J} \tag{3.65}$$

For the 30 kW/6 s discharge capacity, the number of required elements would be

$$N_{\text{batt\_theoric}} = \frac{180{,}000\ \text{J}}{27{,}324\ \text{J}} = 6.58 \Rightarrow 7 \tag{3.66}$$

with a voltage of the whole battery of

$$U_{\text{stack\_theoric}} = 7 \cdot 3.3\ \text{V} = 23.1\ \text{V} \tag{3.67}$$

the corresponding current of the 30 kW discharge being

$$I_{\text{stack\_theoric}} = \frac{30\ \text{kW}}{23.1\ \text{V}} = 1298\ \text{A} \tag{3.68}$$

This value of current is around 10 times the admissible battery current!
The design of the battery pack must be oversized. In order to reduce the current to an acceptable value, the number of elements is multiplied by 10, leading to

$$U_{\text{stack}} = 70 \cdot 3.3\ \text{V} = 231\ \text{V} \tag{3.69}$$

$$I_{\text{stack}} = \frac{30\ \text{kW}}{231\ \text{V}} = 129.8\ \text{A} \tag{3.70}$$

The efficiency of the discharge at 30 kW becomes

$$\eta_{\text{batt\_30}} = \frac{U_{\text{stack}} - R \cdot I_{\text{stack}}}{U_{\text{stack}}} = \frac{231\ \text{V} - 70 \cdot 10 \cdot 10^{-3}\ \Omega \cdot 129\ \text{A}}{231\ \text{V}} = 0.6 \tag{3.71}$$

The calculations for the current and efficiency at reduced power give

***P* [kW]**	***I* [A]**	**η [p.u.]**
15	65	0.8
6	26	0.92
3	13	0.96

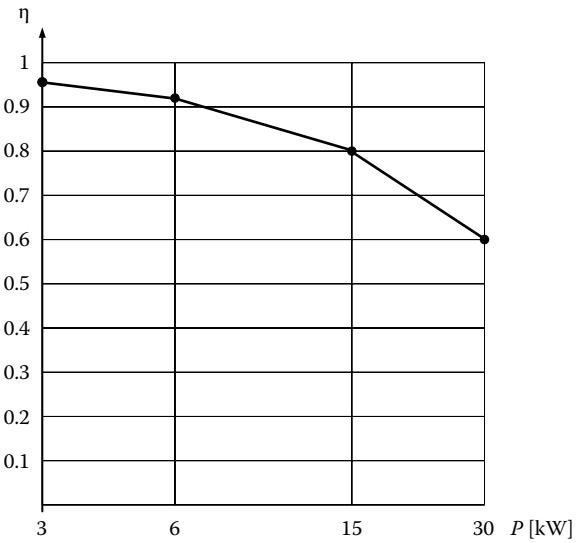

FIGURE 3.26 Efficiency (MRR) of the discharge of the Li-ion-battery-based storage device.

The values of the efficiency are represented in the diagram of Figure 3.26.

The representations of the efficiencies in Figures 3.25 and 3.26 are a good illustration of the performances of the storage devices, and highlight the differences between the two technologies. In opposition to the properties of the supercapacitor-based design, where the efficiency is over 96% in the whole range of operation (power), the design with the Li-ion battery presents problematic energy efficiency values for the upper range of the operation power (0.6 at rated power).

REFERENCES

1. Brunet, Y., *Energy Storage*, ISTE Ltd/John Wiley & Sons, Inc., London, U.K./Hoboken, NJ, 2011.
2. International Electrotechnical Commission (IEC), Letter symbols including conventions and signs for electrical technology, IEC 60027-2, 2005.
3. Magali, R., Solar impulse, Encyclopaedia Universalis [online], http://www.universalis.fr/encyclopedie/solar-impulse/. Accessed on July 21, 2017.
4. Vaclac, S., *Power Density: A Key to Understanding Energy Sources and Uses*, The MIT Press, Cambridge, MA, 2015.
5. Gérard, M., Condensateurs utilisés en électronique de puissance, Techniques de l'ingénieur, Art. Ref: D3010 V1, August 10, 2007.
6. Christen, T., Carlen, M.W., Theory of Ragone plots, *Journal of Power Sources*, 91, 210–216, 2000.
7. Delalay, S., Etude systémique pour l'alimentation hybride—Application aux systèmes intermittents, PhD Thesis No. 5768, EPFL, Lausanne, Switzerland, 2013. https://infoscience.epfl.ch/record/187365/files/EPFL_TH5768.pdf. Accessed on September 22, 2017.

8. Poss, J., Satwicz, J., Richmond, B., Taylor, M., Solar powered compaction apparatus, U.S. Patent 7 481 159 B2, Seahorse Power Company, Needham, MA, January 27, 2009.
9. Barrade, P., Delalay, S., Rufer, A., Direct connection of supercapacitors to photovoltaïc panels with on-off maximum power point tracking, *IEEE Transactions on Sustainable Energy*, 3(2), 283–294, 2012.
10. Culcu, H. et al., Internal resistance of cells of lithium battery modules with FreedomCAR model, *EVS24 and World Electric Vehicle Journal*, 3, 1–9, 2009.
11. DiOrio, N., Dobos, A., Janzou, S., Economic analysis case studies of battery energy storage with SAM. Technical Report, NREL TP-6A20-64987, National Renewable Energy Laboratory (NREL), Golden, CO, November 2015.
12. Klaus, D., Redox-Flow_Batterie: Weniger als 1000 Euro pro kWh Kapazität, Forschung, November 17, 2016. energyload.eu.
13. Rufer, A., Barrade, P., Correvon, M., Weber, J.-F., Multiphysic modelling of a hybrid propulsion system for a racecar application, *EET-2008 European Ele-Drive Conference. International Advanced Mobility Forum*, Geneva, Switzerland, March 11–13, 2008.